The Cryosphere Discuss., 6, 4171–4203, 2012
www.the-cryosphere-discuss.net/6/4171/2012/
doi:10.5194/tcd-6-4171-2012

The Cryosphere
Discussions

Inhomogeneous snow distribution and depletion patterns at grid scale in a shallow snowpack region

H. Li, J. Wang, Z. Tang, and J. Wang

Cold and Arid Regions Environmental and Engineering Research Institute,
Chinese Academy of Sciences, Lanzhou, China

Received: 3 September 2012 – Accepted: 10 September 2012 – Published: 1 October 2012

Correspondence to: H. Li (lihongyi@lzb.ac.cn)

Published by Copernicus Publications on behalf of the European Geosciences Union.

Abstract

Understanding inhomogeneous snow processes at the grid scale is crucial for distributed snow hydrology research. Many studies on inhomogeneous snow processes focus on the annual similarity of snow distribution and depletion and the roles of topography and other environmental conditions. In contrast, this study examines the snow distribution and depletion patterns at a small grid scale in a shallow snowpack region and analyzes how meteorological factors influence these patterns by using the SNOWPACK model for scenario simulations. These simulations enable quantification of the role of three main meteorological factors: shortwave radiation, longwave radiation, and air temperature. The study region is located in the Northeastern Qinghai-Tibet plateau. The results of the study indicate the following two points. (1) During different snowmelt periods, spatial similarity exists between the periodical cumulative snow distributions, and the relationships between snow cover fraction and mean snow water equivalent are similar. However, this similarity is not applicable to the period before snowmelt. (2) Shortwave radiation has a major impact on the snow distribution and depletion patterns at the small grid scale. Increasing shortwave radiation can greatly promote the heterogeneity of the snow distribution. The contributions of longwave radiation and air temperature to the heterogeneity of snow distribution are minor. Moreover, there are similarities between the simulated snow distributions when considering the scenarios of increases in longwave radiation or in air temperature.

1 Introduction

In many studies for modeling distributed snowpack, snowmelt processes at the grid scale are always represented by the simulated results from a point-scale model because of the limited spatial resolution of the forcing data. However, the heterogeneity of snow distribution and melt are important for understanding snow processes at the grid scale, especially in mountainous regions. The influencing factors contributing to the heterogeneity include the terrain conditions (such as slope and aspect), underlying vegetation, solar radiation, and wind (Essery and Pomeroy, 2004; Schirmer et al., 2011). For all these uncertain environmental factors, the modeling accuracy is heavily influenced by the model's spatial resolution and the described physical details of the snow model at the grid scale. Some research studies have demonstrated that simulated results vary significantly when using different model grid scales (Cline et al., 1998; Hebeler and Purves, 2008). Determining an appropriate description of heterogeneous snow processes at the grid scale has attracted more attention recently.

To understand inhomogeneous snow processes at the grid scale, researchers (Skaugen and Randen, 2011; Schirmer et al., 2011) usually investigate certain statistical indicators, such as the mean Snow Water Equivalent (SWE), Standard Deviation (SDV) and Coefficient of Variation (CV), to quantitatively express the snow distribution. In most cases, it is difficult to investigate each grid in a large-scale basin or an interesting region. Instead, researchers usually use more operational empirical methods to evaluate interesting objectives, such as the mean SWE. These methods mainly refer to the repeated snow cover depletion patterns, which occur seasonally because of the changeless underlying conditions and terrains. For example, Donald et al. (1995) indicated that the maximum snow accumulation height could be regarded as a function of vegetation height and topography and that the snowpack changes with consistent patterns annually. A more general method to describe the heterogeneity is to use the Snow cover Depletion Curve (SDC), which represents a nonlinear relationship between the Snow Cover Fraction (SCF) and the SWE at the grid scale (Essery and Pomeroy, 2004). Some researchers have utilized repeated patterns and a snow model to determine the snow distribution (Sturm and Wagner, 2010). The SDCs should be regionally used only after being calibrated because of the inhomogeneous terrain, vegetation and other regional factors of influence. Some researchers (Kolberg and Gottschalk, 2010) have studied the interannual stability of grid cell SDCs by using satellite data.

The snow distribution and depletion patterns at the grid scale require further study in the following aspects. First, the influence of different meteorological factors on the heterogeneity of snow depletion and distribution has rarely been mentioned. Snowpack ablation is the result of a combination of meteorological force inputs and terrain conditions. Some inputs, such as solar radiation, are heavily dependent on the slope and the aspect (Liston and Elder, 2006), while other energy inputs, such as turbulent fluxes, are more dependent on the micro-topography and the underlying snow surface. The snow distribution is not only influenced by terrain factors but is also influenced by different meteorological data that change daily and seasonally. It is interesting and necessary to study this combination of effects to better understand snow processes at the grid scale. Second, it is necessary to analyze the seasonal statistical features of snow distribution at the grid scale. Most prior studies have assumed that a single SDC can offers an adequate description of the snow distribution (Shamir and Georgakakos, 2007). However, the real SDC changes under different temporary weather conditions. A permanent snow depletion pattern is almost never observed in any snow-covered region during a time series of snowpack evolution. Third, many previous studies have focused on those regions with thick snowpack. However, the snow distribution is more unstable in shallow and fractional snowpack regions such as the Tibetan Plateau (Shreve et al., 2009). Thus, in these shallow snowpack regions, it is likely that the snow patterns are much different than those observed in previous studies.

What snow distribution and depletion patterns exist at the grid scale in a shallow snowpack region? How do meteorological factors influence these patterns during different snow seasons?

The objective of this paper is to address these questions by a combination of field observations and a physics-based snow model. The contents include the following: (1) an investigation of the statistical indicators of snow distribution at the grid scale by accurate field observations; (2) the modeling of the energy and mass exchange of snowpacks at the grid scale; (3) an analysis of the possible influence of meteorological data on snow processes based on the combination of observations and scenario simulations.

2 Methods and data

This research depends on field observations and the SNOWPACK model (Bartelt and Lehning, 2002). First, multi-point snow properties were investigated by a time series of field observations in a grid. Meteorological data were obtained from the Auto Weather Station (AWS) located in the study region. Second, the SNOWPACK model was used to simulate scenarios of snowpack changes in the grid. Using the observations and the model, the influence of different factors on the snow distribution and depletion patterns during different snow seasons was analyzed based on the calibrated model and the observational results. The following is a detailed description of the field observations, the SNOWPACK model, and the method of analysis for the snow distribution and depletion patterns.

2.1 Field observation

The study region is situated in the Qilian mountainous region of the Northeastern Qinghai-Tibet plateau (Li et al., 2009; Li and Wang, 2011). Seasonal snow is prevalent in this region. Most of the snowfall occurs in autumn and spring. The snow cover is primarily shallow and patchy.

The selected study grid is located in a gradual north slope, with alpine meadows and a few bushes (Fig. 1). The altitude of the selected region is approximately 3260 m. The grid had dimensions of 100 m by 100 m and was divided into 100 sub-grids with a resolution of 10 m. There were 121 sampling points for the 100 sub-grids. The coordinates of these sampling points were measured by a total station instrument. Snow properties such as depth and density were measured at each of the points during a snow season from November 2011 to March 2012. The snow depth was repeatedly measured four times in four different directions at each sampling point. The measured snow depths at the sampling points located in the four corners were averaged to determine the snow depth of each sub-grid. The start time of the daily field observation was 10 a.m. The daily observation duration was approximately 2 h.

There is an AWS in the upper left of the study grid, which measures the 30-min downward/upward shortwave/longwave radiation, wind speed/direction, air temperature, relative humidity, precipitation, snow depth and snow water equivalent.

2.2 SNOWPACK model

SNOWPACK is a one-dimensional physical snowpack model used to simulate the snow surface energy exchange, mass balance, snowpack settlement and layering (Lehning et al., 2002; Bartelt and Lehning, 2002; Fierz et al., 2003). This model is widely used in many snow studies and has produced reliable results in applications around the world (Stössel et al., 2010; Lehning et al., 2006). By using the model, we can obtain some of the required variables, such as the different energy inputs of the snowpack and the modeled SWE. In this paper, the SNOWPACK model was used for the analysis of scenarios for the snow distribution and depletion patterns.

We chose the period from 9 February to 21 March 2012 as the simulation duration. This period was primarily chosen to ensure the snowpack underwent a complete process, including accumulation and ablation. In addition, intensive measurements were made for model calibration and to obtain the real precipitation distribution during this period.

To model the snowpack change at each sub-grid in the study grid, SNOWPACK was repeatedly run 100 times using different altitudes, slopes, aspects and vegetation heights. There are various methods for choosing the force inputs for the SNOWPACK model (Bartelt and Lehning, 2002). For the best simulation results, as many inputs as possible were chosen, including incoming shortwave radiation, incoming longwave radiation, wind speed, air temperature, and relative humidity. Because the grid size is small (100 m × 100 m), it is assumed that the measured force inputs (radiation, air temperature, wind speed and relative humidity) are the same over the 100 grids at each horizontal level. Of course, the horizontal radiation was adjusted for the different aspects and slopes by the model itself.

Inhomogeneous precipitation data were obtained from the field snow measurements before and after the occurrence of precipitation. A few days did not include in-situ measurements. For calculating the precipitation distribution in these days, we note these days as an A day, and chose a nearest day which has measurement, noted as a B day. Then we calculated the spatial ratio of the distributed precipitation to the observed precipitation at the AWS in B day. Next, the ratio of the A day was assumed to be the same as that of the B day, and the current precipitation distribution of the A day could be obtained by the ratio by multiplying the real precipitation at the AWS. Because the size of the study grid is small, it is assumed the precipitation distribution has no strong heterogeneity, then the ratio was restricted to the range of 0.8 to 1.2.

In this study, the outputs of SNOWPACK included detailed values of the snow properties and the exchanges of energy and mass. This study focused on the modeled SWE distribution. SCF was calculated by dividing the number of sub-grids, which modeled the existing snow, by the total number of sub-girds in the study grid.

2.3 Quantitative description of the snow distribution and depletion patterns

Two methods were used in this paper to describe the snow distribution and depletion patterns. The first method was to analyze the spatial similarity of the snow distributions in different periods. For this purpose, the concept of the spatial accumulation factor was used to describe the weight of each sub-grid SWE relative to the average SWE over the total grid. In addition, we used a Probability Density Function (PDF) to describe the probability distribution of the in-situ measured SWE for all of the sub-grids. By determining PDF families during a snow season, the snow cover depletion processes can be quantitatively described and analyzed.

The second method was to compare the relationships between certain variables (such as the mean SWE vs. SCF and the mean SWE vs. SDV) in different periods. In many previous studies, the SDC, which represents the relationship between SWE and SCF, was used to describe the snow depletion pattern. In addition, to compare the heterogeneity of snow distributions in different periods, the relationship between SWE and SDV was analyzed.

The following is a detailed description of the calculation of the spatial accumulation factor and of the use of the PDF of the snow distribution.

2.3.1 Spatial accumulation factor

We want to determine the spatial features of continuous snow change during a specific period, such as the winter accumulation period or the spring melt period. A Periodical Accumulation Factor (PAF) was used to describe the periodical cumulative snow distributions.

$$\mathrm{PAF}_{t1-t2}(x,y)=\frac{\sum\limits_{t=t1}^{t2}\mathrm{SWE}_t(x,y)}{\sum\limits_{t=t1}^{t2}\overline{\mathrm{SWE}_t}} \tag{1}$$

where $t1$ and $t2$ are the start time and end time, respectively, of a specific period. $\overline{\mathrm{SWE}_t}$ is the averaged SWE value throughout the grid at day t, and x and y are the relative coordinates of the sub-grid.

To analyze the similarity between the SWE distributions of different days, the coefficient of correlation was calculated by the following equation,

$$\rho=\frac{1}{n}\cdot\frac{\sum\limits_{i=1}^{n}(\mathrm{SWE}_i^{t1}-E(\mathrm{SWE}^{t1}))(\mathrm{SWE}_i^{t2}-E(\mathrm{SWE}^{t2}))}{\sigma(\mathrm{SWE}^{t1})\cdot\sigma(\mathrm{SWE}^{t2})} \tag{2}$$

where n is the number of total sub-grids, and SWE_i^{t1} (SWE_i^{t2}) is the SWE at sub-grid "i" at $t1$ ($t2$) day. $E(\mathrm{SWE}^{t1})$($E(\mathrm{SWE}^{t2})$) is the expected value of all SWE values at $t1$ ($t2$) day. $\sigma(\mathrm{SWE}^{t1})$($\sigma(\mathrm{SWE}^{t2})$) is the variance of all SWE values at $t1$ ($t2$) day.

In Eq. (2), SWE can be replaced by PAF if the similarity of snow depletion patterns is to be evaluated between different durations.

2.3.2 PDF of the snow distribution

In recent studies, a lognormal distribution (Donald et al., 1995) or a gamma distribution (Skaugen, 2007) was typically used to represent the SWE distribution. No significant difference was determined between these two distributions in an examination with field samplings. A lognormal distribution was chosen in this study to describe the PDF of the snow distribution (Donald et al., 1995),

$$f(\mathrm{SWE},\mu,\sigma) = \frac{1}{\sqrt{2\pi}(\mathrm{SWE})\sigma} \exp\left[-\frac{(\ln(\mathrm{SWE})-\mu)^2}{2\sigma^2}\right] \tag{3}$$

$$\mu = \ln(E(\mathrm{SWE})) - \frac{1}{2}\ln\left(1 + \frac{\mathrm{Var(SWE)}}{E(\mathrm{SWE})^2}\right) \tag{4}$$

$$\sigma^2 = \ln\left(1 + \frac{\mathrm{Var(SWE)}}{E(\mathrm{SWE})^2}\right) \tag{5}$$

In these equations, Var(SWE) is the variance of the SWE distribution, and E(SWE) is the expected value of the SWE distribution. We counted all the SWE values in a grid, after which the PDF was defined.

3 Results

From the field investigation results, the statistical indicators, including SCF, mean SWE, CV and SDV, were calculated. The daily SWE values were fitted to lognormal distributions using the estimators (E(SWE) = mean SWE, VAR(SWE) = SDV^2) according to Eqs. (3–5). The snowpack changes at all sub-grids were modeled using the SNOWPACK model from 9 February to 21 March 2012.

3.1 Snow distribution change

From the field investigation results in November 2011 (Fig. 2), the mean SWE decreased with the gradual decrease of the SCF in the initial duration of the melt, while the mean SWE changed slowly (between 11–12 cm) when the SCF decreased during the later days. The CV exhibited a rapidly increasing trend when snowmelt occurred, and it decreased very slowly afterward. The SDV exhibited a similar trend with the change in the SCF.

As the field investigation results indicated in February and March 2012 (Fig. 3), there are two different periods: the earlier stage with slow accumulation and the later stage with fast ablation. During the earlier stage, the SCF values changed slightly before the beginning of snowmelt, while the SWE increased slowly. Meanwhile, the CV and SDV were nearly unchanged. During the later days (14 March to 21 March), the SCF and SWE decreased drastically with the occurrence of the snowmelt processes. Meanwhile, the CV increased and the SDV decreased rapidly.

With the expected values and variances determined from the field observations, the SWE distribution was fitted by a lognormal distribution. We chose two typical periods to express the results (Fig. 4): November 2011 and March 2012. During March, the expected value decreased and the peak value increased with the snowmelt process. However, a similar trend was not obvious in November 2011.

The above investigation indicated the following: (1) the SWE decreased with the reduction of the SCF during the snowmelt period if the SCF was less than 1; (2) there was no specific functional relationship between SCF and SWE, especially when the grid was fully covered by snowpack, in which case, the SCF value (equal 1) could be mapped to many SWE values, which depended on the earlier snow accumulation; and (3) the CV and SDV values did not exhibit significant changes during winter, when no abundant precipitation or obvious melting occurred. When snowmelt occurred, the CV increased and the SDV decreased.

3.2 Modeled results using the SNOWPACK model

The distributed snow processes were modeled using the SNOWPACK model for multiple points in the grid. The modeled results were assessed by four different estimators: the mean SWE, SCF, SDV and CV (Fig. 5). The Nash–Sutcliffe model efficiency coefficient (Nash coefficient) of the modeled mean SWE is 0.72 and that of the modeled SDV is 0.87, indicating that the modeled results exhibit fine accuracy in the mean value and the standard deviation during the simulated period. Major disagreement with the observed SWE exists in the data from late February. Because the CV is the ratio of the mean SWE to the SDV, a small error of the mean SWE or SDV will lead to a large bias of the CV. The SCFs were reliably simulated throughout the entire simulation period. If the SWE is approximately 0, a large error may exist. Because the SCF value was evaluated by counting the number of sub-grids with snow, it is difficult to accurately distinguish 0 and a very small SWE value.

The results indicated good agreement in the mean value and the heterogeneity of the modeled snow SWE at the grid scale. The results can be reliably used for further analyses and scenario simulations using the calibrated model.

4 Discussion

What are the snow distribution and depletion patterns at the grid scale in this shallow snow region? And how do meteorological factors influence these patterns? We divided the snow season into pre-melt and snowmelt periods, and we discuss the following aspects of these issues: (1) the spatial similarity of the snow distributions during the snowmelt and pre-melt periods; (2) the relationships between different variables (mean SWE vs. SCF and mean SWE vs. SDV) in the two periods and the influence of meteorological factors on these relationships; and (3) the spatial and temporal limitations of the snow distribution and depletion patterns.

4.1 Spatial similarity of the snow distribution and depletion patterns during different snow seasons

4.1.1 Spatial distribution pattern in a pre-melt period

Some studies define the prior snow distribution before the snowmelt period and emphasize a critical time between the pre-melt period and the melt period (Kolberg et al., 2006). If continuous observation of the snowpack distribution is performed before the snowmelt period, then the prior distribution parameters can be defined empirically. In our analysis, we determined if the spatial rules of a prior snow distribution exist in the pre-melt period in our study region.

Because the snowpack is shallow in the study region, it can significantly melt or be sublimated at any time. We divided our study period into three stages: the autumn snowmelt season, the winter snow accumulation season, and the spring snowmelt season. We divided each season into a pre-melt period and a melt period according to three critical times: 6 November 2011, 21 February 2012, and 13 March 2012. Next, we compared the prior snow distributions in these days using a coefficient of correlation (Eq. 2).

The results indicated that there is a weak correlation between the distributions of 6 November and 13 March. The coefficient of correlation is 0.55. There are some similarities between the two SWE distributions (Fig. 6). However, the frequency distributions of the two days are different. A bimodal distribution of frequency was observed on 6 November because of the latest snowfall, while the frequency distribution on 13 March is a unimodal distribution. This difference in frequency distributions is the main reason why the similarity of snow distributions is weak between these two days. We found that the SWE distribution of 21 February is significantly different from the other days (the coefficients of correlation to 6 November and 13 March are 0.13 and 0.19, respectively). In February, due to the very low air temperature (less than $-10\,^{\circ}\mathrm{C}$), the snowpack decreased primarily by sublimation. There is significant difference between the snow distributions in winter and the other snow seasons. In addition, the SDV or CV values obviously changed during these days.

The above analyses demonstrate that the rule of prior distribution is unstable for a shallow snowpack region. Some studies set an initial snow distribution prior to the melt season (Egli et al., 2012), but this approach is obviously unsuitable for a shallow snowpack region at the grid scale. Some researchers (Skaugen, 2007) have noticed a change in the spatial CV during the snow season, with a decreasing trend from the start of the accumulation period and a sharp increase in the melting period. For spatially distributed snow modeling, Liston (2004) defined different CV values for 9 typical snow-distribution categories. These research results provide some directions to consider when dealing with spatial-temporal complexity in understanding the snow distribution during the pre-melt period in a shallow snow region.

4.1.2 Spatial snow distribution and depletion patterns in a snowmelt season

Are there obvious spatial depletion features during a snowmelt period? And are the snow distributions similar when the SCF values are approximately equal? We analyze the spatial snow distribution in two aspects: the first is to compute the coefficient of correlation of two different days that exhibit similar SCF values, and the second is to compare the periodical accumulation factors PAF during different snowmelt periods.

We chose different pairs of snow days with similar SCF values in the period from November 2011 to March 2012. All the coefficients of correlation were determined to be less than 0.5. This low correlation indicates that even with similar SCF values, the spatial correlation of the snow distribution of these days is weak. This weak correlation is primarily due to the shallow snowpack in this region. With a small snowmelt or blowing snow, the snow distribution can rapidly change in this region.

To compare the periodical accumulation of the snow distributions in a snow period, we chose two periods, 6 November 2011 to 11 November 2011 and 13 March 2012 to 21 March 2012, and compared the periodical accumulation factors of the two periods using Eq. (2).

The results (Fig. 7) indicate excellent agreement between the two periods. The coefficient of correlation of the two PAF matrices is 0.76. The obvious difference is denoted in Fig. 7 by a white circle. In this circle, there are high values in 2011, which are different from the data in 2012. According to the in-situ observation, we noticed that there are occasional blowing snow events from 4 March to 7 March. The SDV and CV changed suddenly during these days (Fig. 3). These blowing snow events affected the prior distribution, especially in the circled region before the snowmelt season. The results indicate that the snow distribution and depletion patterns during the snowmelt season can be influenced by the prior distribution; however, the periodical accumulation factor still exhibits a stable spatial pattern.

Note that this stable spatial pattern only exists in a snowmelt period. To illustrate this point, we compared the periodical accumulation factors between February 2012 and March 2012 (or November 2011) and found that the correlation is very small. The reason for this poor correlation is that the snowpack distribution became more homogeneous in February because there were no dramatic snowmelt events during this period. The spatial depletion pattern in this period is obviously different from those during the snowmelt seasons.

The above discussion indicates that a stable snow distribution and depletion pattern exists in different snowmelt periods. This stable pattern is obvious even in a shallow snowpack region, although it was slightly affected by the prior snow distribution before the snowmelt period.

4.2 Relationship between the mean SWE and the SCF (or SDV)

First, we examined the relationships between the in-situ measured mean SWE and SCF or SDV in the different periods. Furthermore, we analyzed the responses of these relationships to different meteorological scenarios by using the calibrated SNOWPACK model.

4.2.1 Results from the field investigation

The relationships between the mean SWE and the SCF are similar in two different snowmelt periods (November 2011 versus March 2012) (Fig. 8). Note that there is growing uncertainty in the relationship between the mean SWE and the SCF when the SCF is at or near 100 %. A snowfall with any intensity can cover the entire grid, so there are many possible SWE values corresponding to a SCF at or near 100 %. In our study, there is a series of SWE values with a loose range when the SCF is greater than 0.9 (Fig. 8). The SCF decreases gradually with the snowmelt process, and the relationship between the SCF and the mean SWE exhibits a certain trend.

There is no obvious similarity between the mean SWE and the SDV in the different periods. Only seasonal features can be found in the scatter plot between the mean SWE and the SDV (Fig. 8). The SDV values are higher in the snowmelt periods (November 2011 and March 2012), while they are lower during winter (February 2012), when snowmelt events are rare. The results indicate that the heterogeneity of the snow distribution is relatively larger when the snowmelts are significant.

4.2.2 Influence of meteorological factors on the snow depletion pattern

The features of the snow distribution and depletion are formed from the interaction between meteorological factors and environmental conditions. We have discussed the similarity of the snow distribution and depletion patterns in different periods. However, these real situations are not sufficient to analyze the influences of different meteorological factors on the spatial patterns. Thus, we established a series of scenario simulations using the SNOWPACK model to understand the potential influences of different types of meteorological factors on the relationships between the mean SWE and the SCF (or SDV).

We set three main meteorological factors in the model: incoming shortwave radiation, incoming longwave radiation and air temperature. The following are the different designed scenarios, in which only one factor was adjusted in the input force dataset for the SNOWPACK model.

1. Analyzing the response to shortwave radiation change. The hourly incoming shortwave radiation input increased by 30 W, 60 W and 90 W, while the other factors remained unchanged.
2. Analyzing the response to longwave radiation change. The hourly incoming longwave radiation input increased by 30 W, 60 W and 90 W, while the other factors remained unchanged.
3. Analyzing the response to air temperature change. The hourly air temperature input increased by 5 K, 10 K and 15 K, while the other factors remained unchanged.

The scenario simulations indicated that incoming shortwave radiation can significantly affect the heterogeneity of the snow distribution at the grid scale. In the increasing shortwave radiation scenarios, the snowpack melt increased and the SCF sharply decreased (Fig. 9). No remarkable regularity is observed in the scatter plot between the mean SWE and the SCF in the different scenarios. The SDV values increased and their range expanded with the increase in the incoming shortwave radiation. The heterogeneity of the snow distribution obviously increased. This result is in agreement with our prior knowledge that shortwave radiation is closely related to topography. On a slope, shortwave radiation primarily comes from direct radiation and partially from scattered radiation. The direct shortwave radiation depends on the slope and the aspect. In the assumed scenarios, the increase of the shortwave radiation melted more snowpack on the south-facing slopes, which receive more radiation, thereby increasing the heterogeneity of the snow distribution. The snow cover depletion pattern heavily depends on the topography because of the redistribution of shortwave radiation on the slopes.

Incoming longwave radiation has a minor impact on the heterogeneity of the snow distribution at the grid scale. The snowpack melt increased and the SCF decreased when the incoming longwave radiation increased, in a manner similar to the scenario of the increasing shortwave radiation. However, the increase of longwave radiation was not found to significantly contribute to the heterogeneity of the snow distribution. The scatter plots between the mean SWE and the SCF remained close for the different scenarios of longwave radiation change, and the SDV values changed over a small range (Fig. 10). These results suggest that some regularity exists in the relationship between the mean SWE and the SCF in the different scenarios of increasing longwave radiation in our grid region. In addition, the SCF reaches 0 when the incoming longwave radiation increases, while the minimum SCF value is 0.3 in the scenarios of shortwave radiation change. This result indicates that the snow distribution changes in different manners by shortwave radiation versus longwave radiation when its quantities are the same. Slope is the main topographical factor influencing longwave radiation, while aspect exhibits nearly no effect on it. Thus, the heterogeneity of longwave radiation is less than that of shortwave radiation in our study region. Longwave radiation causes the snow depletion pattern to be more spatially homogeneous.

The heterogeneity of the snow distribution does not exhibit a significant increase in the scenarios of air temperature change. The change of the relationship between the mean SWE and the SCF is not obvious when the air temperature increases (Fig. 11). In addition, there is some regularity in the relationship between the mean SWE and the SCF in the different scenarios of increasing air temperature. The SDV values exhibit a smaller change than in those scenarios of increasing longwave radiation, and the values cover a small range. In the small scale grid, the air temperature exhibits nearly no spatial heterogeneity.

In summary, for the small grid, the heterogeneity of the shortwave radiation scenario is the most significant, that of the longwave radiation scenario is weak, and that of the air temperature scenario can be ignored. The different scenario simulations indicate that the heterogeneity of the snow distribution depends heavily on the incoming shortwave radiation, which obviously influences the snow depletion pattern. The contributions from incoming longwave radiation and air temperature are relatively weak.

The snow distribution and depletion patterns exhibit some regularity when incoming longwave radiation or air temperature is changed.

4.3 The spatial-temporal limitation of the snow distribution and depletion patterns

We analyzed how meteorological factors affect the snow distribution and depletion patterns at the grid scale in a shallow snowpack region. The regularity of the spatial snow depletion is heavily dependent on the seasonal features of the meteorological factors. For example, lower values of shortwave radiation and air temperature are present in winter and are higher in spring. This seasonality leads to the temporal limitation for the spatial pattern of snow depletion. Note that some stochastic factors will occasionally affect these patterns. For example, if more cloudy days occurred than did a year earlier or if an anomalous snowfall occurred, then the snow depletion pattern will be affected. Because blowing snow is not frequent in our study region, we have not highlighted the influence of blowing snow. In some blowing snow-dominated regions, the snow depletion pattern would be more complex because of the redistribution of the snowpack by wind.

Topography is the other important factor in determining the snow distribution and depletion patterns. Because the grid scale is small and the topography is relatively uniform in our study region, some of the forcing data, such as air temperature, are nearly homogeneous. In more complex terrain conditions, the uncertainty from meteorological factors will be significantly higher. The dominant forces forming the snow depletion pattern are very different over different grid scales. At large scales, such as from 10 to 1000 km, the snow distribution features depend on the latitude, elevation, and terrain and the presence of large water bodies. Because of the limitation of our research target and the measurement capacity, the grid size we chose was small (100 m by 100 m). If a larger scale is considered, additional force factors should be studied.

In addition, in our study region, the snowpack is shallow and there is almost no prolonged snow accumulation or melt period. In some regions with thick snowpack, researchers (Schirmer et al., 2011) have observed that the patterns of maximum accumulation are similar in different snow periods. No similar regularity is observed in our study region. Slight snowmelt or snowfall could result in a significant change of the snow distribution. The snow distribution and depletion pattern is expected to be more stable in regions with a thick snowpack than those with a shallow snowpack.

5 Conclusion

Snow distribution and depletion patterns at the small grid scale were investigated by in-situ measurements and a physics-based snow model in a shallow snowpack region on the Northeastern Qinghai-Tibet plateau. The modeled mean SWE and standard deviation of the spatial snow processes exhibited excellent agreement with the observed values. Inhomogeneous spatial snow processes were analyzed, and the influences of meteorological factors on the heterogeneity of the spatial snow processes were discussed.

In the study region, the investigation indicated that snow distribution and depletion exhibit obvious seasonal features. There is remarkable similarity between the periodical snow accumulation distributions in different snowmelt periods, but this similarity could not be applied to the entire snow season. In the pre-melt period, there is no similarity between the periodical snow accumulation distributions in the shallow snowpack region. The correspondence between the mean SWE and the SCF exhibits some regularity in different snowmelt periods. It is possible that in the snowmelt period, the mean SWE or SCF could be evaluated using these regularities. There is no marked similarity, but rather seasonal differences, between the relationships of the mean SWE and the SDV in the different pre-melt and snowmelt periods.

The roles of meteorological factors in forming the snow distribution and depletion patterns are different from each other. The results of the scenario simulations indicate that the snow distribution and depletion patterns at the grid scale heavily depend on the shortwave radiation. Increased shortwave radiation is found to significantly promote the heterogeneity of the snow distribution. The contributions to the heterogeneity from longwave radiation and air temperature are small. Some regularity exists in the scenarios where longwave radiation or air temperature is increased.

The results from this paper can be applied to further studies of the inhomogeneous snow processes in shallow or patchy snowpack regions. Other factors not emphasized in the paper, such as the grid scale and a thicker snowpack, should be further considered according to the actual situations in the study of the snow distribution and depletion patterns in other regions.

Acknowledgements. The authors acknowledge Michael Lehning, Charles Fierz and Mathias Bavay from WSL Institute for Snow and Avalanche Research SLF for providing the SNOWPACK model and guidance for simulation. This work has been founded by the CAS (Chinese Academy of Sciences) Action Plan for West Development Project (grant no: KZCX2-XB3- 15), the National Natural Science Foundation of China (grant no: 41001240) and the FP7 project CEOP-AEGIS (grant no.212921).

References

Bartelt, P. and Lehning, M.: A physical SNOWPACK model for the Swiss avalanche warning: Part I: numerical model, Cold Reg. Sci. Technol., 35, 123–145, 2002.

Cline, D., Elder, K., and Bales, R.: Scale effects in a distributed snow water equivalence and snowmelt model for mountain basins, Hydrol. Process., 12, 1527–1536, 1998.

Donald, J. R., Soulis, E. D., Kouwen, N., and Pietroniro, A.: A land cover-based snow cover representation for distributed hydrologic-models, Water Resour. Res., 31, 995–1009, 1995.

Egli, L., Jonas, T., Grünewald, T., Schirmer, M., and Burlando, P.: Dynamics of snow ablation in a small Alpine catchment observed by repeated terrestrial laser scans, Hydrol. Process., 26, 1574–1585, doi:10.1002/hyp.8244, 2012.

Essery, R. and Pomeroy, J.: Implications of spatial distributions of snow mass and melt rate for snow-cover depletion: theoretical considerations, Ann. Glaciol., 38, 261–265, 2004.

Fierz, C., Riber, P., Adams, E. E., Curran, A. R., Föhn, P. M. B., Lehning, M., and Plüss, C.: Evaluation of snow-surface energy balance models in alpine terrain, J. Hydrol., 282, 76–94, doi:10.1016/s0022-1694(03)00255-5, 2003.

Hebeler, F. and Purves, R. S.: The influence of resolution and topographic uncertainty on melt modelling using hypsometric sub-grid parameterization, Hydrol. Process., 22, 3965–3979, doi:10.1002/hyp.7034, 2008.

Kolberg, S. and Gottschalk, L.: Interannual stability of grid cell snow depletion curves as estimated from MODIS images, Water Resour. Res., 46, W11555, doi:10.1029/2008wr007617, 2010.

Kolberg, S., Rue, H., and Gottschalk, L.: A Bayesian spatial assimilation scheme for snow coverage observations in a gridded snow model, Hydrol. Earth Syst. Sci., 10, 369–381, doi:10.5194/hess-10-369-2006, 2006.

Lehning, M., Bartelt, P., Brown, B., and Fierz, C.: A physical SNOWPACK model for the Swiss avalanche warning: Part III: meteorological forcing, thin layer formation and evaluation, Cold Reg. Sci. Technol., 35, 169–184, 2002.

Lehning, M., Voelksch, I., Gustafsson, D., Nguyen, T. A., Staehli, M., and Zappa, M.: ALPINE3D: a detailed model of mountain surface processes and its application to snow hydrology, Hydrol. Process., 20, 2111–2128, doi:2110.1002/hyp, 2006.

Li, H.-Y. and Wang, J.: Simulation of snow distribution and melt under cloudy conditions in an Alpine watershed, Hydrol. Earth Syst. Sci., 15, 2195–2203, doi:10.5194/hess-15-2195-2011, 2011.

Li, X., Li, X., Li, Z., Ma, M., Wang, J., Xiao, Q., Liu, Q., Che, T., Chen, E., Yan, G., Hu, Z., Zhang, L., Chu, R., Su, P., Liu, Q., Liu, S., Wang, J., Niu, Z., Chen, Y., Jin, R., Wang, W., Ran, Y., Xin, X., and Ren, H.: Watershed allied telemetry experimental research, J. Geophys. Res., 114, D22103, doi:10.1029/2008jd011590, 2009.

Liston, G. E.: Representing subgrid snow cover heterogeneities in regional and global models, J. Climate, 17, 1381–1397, 2004.

Liston, G. E. and Elder, K.: A meteorological distribution system for high-resolution terrestrial modeling (MicroMet), J. Hydrometeorol., 7, 217–234, 2006.

Schirmer, M., Wirz, V., Clifton, A., and Lehning, M.: Persistence in intra-annual snow depth distribution: 1. Measurements and topographic control, Water Resour. Res., 47, W09516, doi:10.1029/2010wr009426, 2011.

Shamir, E. and Georgakakos, K. P.: Estimating snow depletion curves for American River basins using distributed snow modeling, J. Hydrol., 334, 162–173, doi:10.1016/j.jhydrol.2006.10.007, 2007.

Shreve, C. M., Okin, G. S., and Painter, T. H.: Indices for estimating fractional snow cover in the Western Tibetan Plateau, J. Glaciol., 55, 737–745, 2009.

Skaugen, T.: Modelling the spatial variability of snow water equivalent at the catchment scale, Hydrol. Earth Syst. Sci., 11, 1543–1550, doi:10.5194/hess-11-1543-2007, 2007.

Skaugen, T. and Randen, F.: Modelling the spatial distribution of snow water equivalent at the catchment scale taking into account changes in snow covered area, Hydrol. Earth Syst. Sci. Discuss., 8, 11485–11518, doi:10.5194/hessd-8-11485-2011, 2011.

Stössel, F., Guala, M., Fierz, C., Manes, C., and Lehning, M.: Micrometeorological and morphological observations of surface hoar dynamics on a mountain snow cover, Water Resour. Res., 46, W04511, doi:10.1029/2009wr008198, 2010.

Sturm, M. and Wagner, A. M.: Using repeated patterns in snow distribution modeling: an Arctic example, Water Resour. Res., 46, W12549, doi:10.1029/2010wr009434, 2010.

Title Page
Abstract
Introduction
Conclusions
References
Tables
Figures
◀▌
▶▌
◀
▶
Back
Close
Full Screen / Esc
Printer-friendly Version
Interactive Discussion

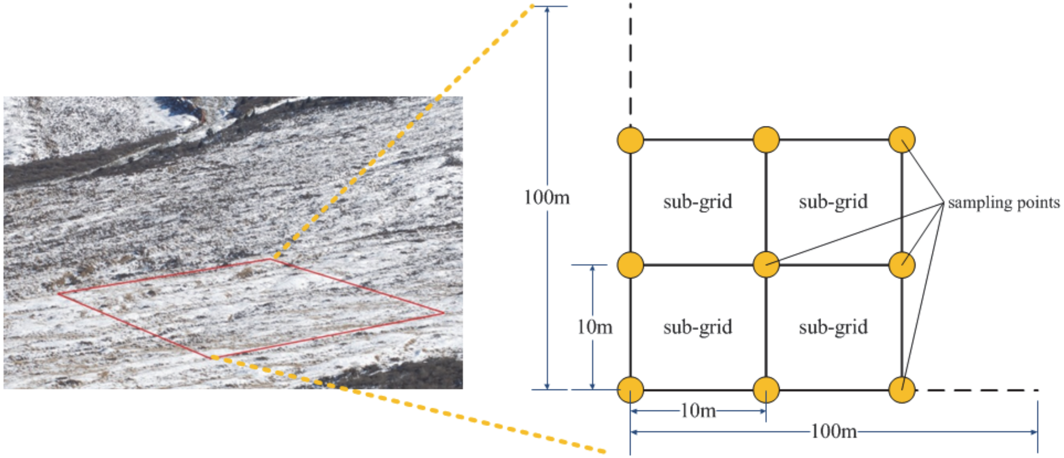

Fig. 1. The study region grid, with a resolution of 100 m by 100 m. The study region is located in Northeastern Qinghai-Tibet. The grid was divided into 100 sub-grids with a 10 m resolution. Each sub-grid has four sampling points located in the four corners.

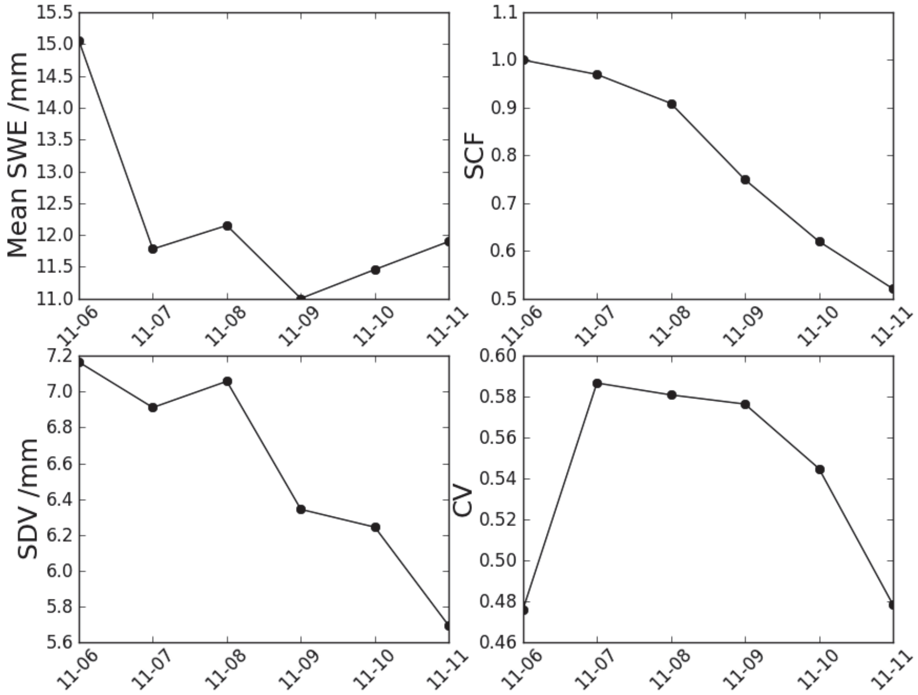

Fig. 2. Observed parameters, including the SCF, mean SWE, CV and SDV, from 6 November to 11 November 2011. These parameters were calculated from field samplings over 100 sub-grids.

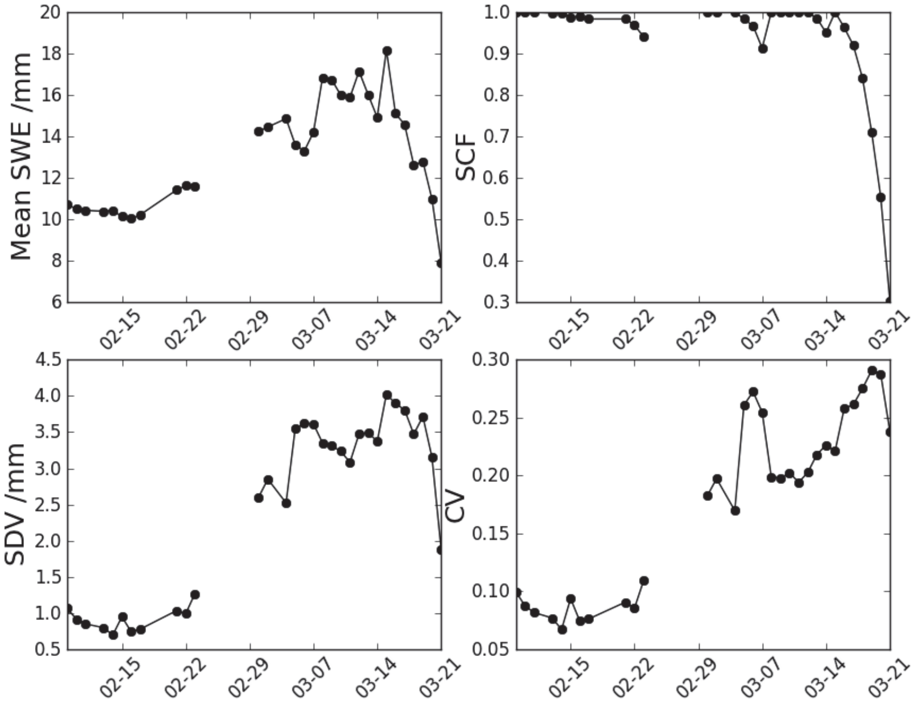

Fig. 3. Observed parameters, including the SCF, mean SWE, CV and SDV, from 9 February to 21 March 2012. These estimators were calculated from field samplings over 100 sub-grids. There is a gap in the observations between 24 February and 29 February.

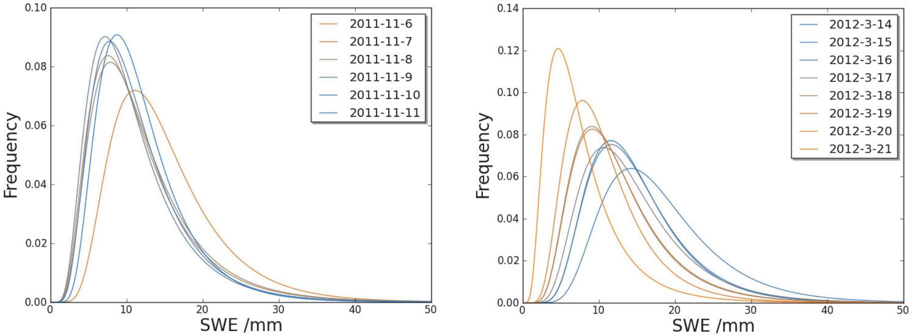

Fig. 4. PDFs of the investigated SWE distributions during two snowmelt seasons: November 2011 (left) and March 2012 (right).

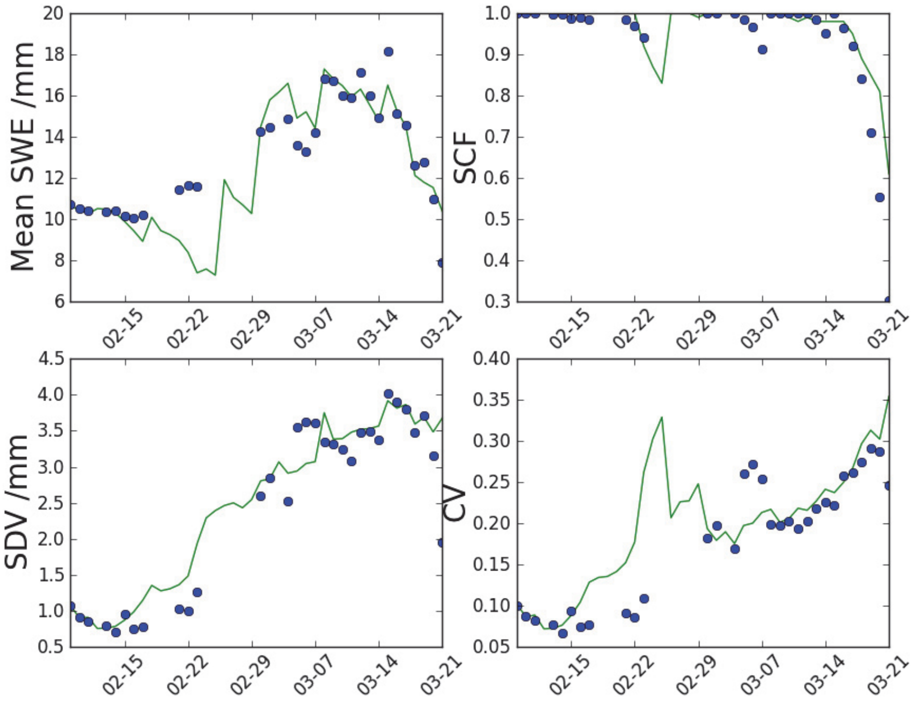

Fig. 5. Modeled mean SWE, SDV, SCF and CV at the grid scale from 9 February to 21 March, 2012.

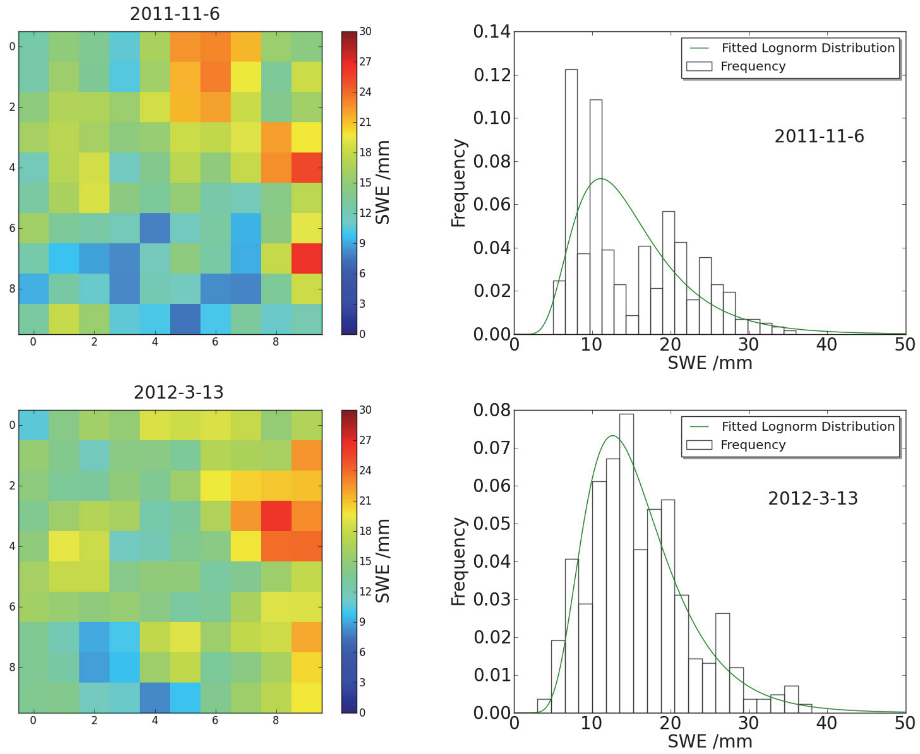

Fig. 6. Investigated SWE distributions for two critical days (6 November 2011 and 13 March 2012). The right is the frequency of the SWE distribution of each day. The data were fitted using a lognormal distribution.

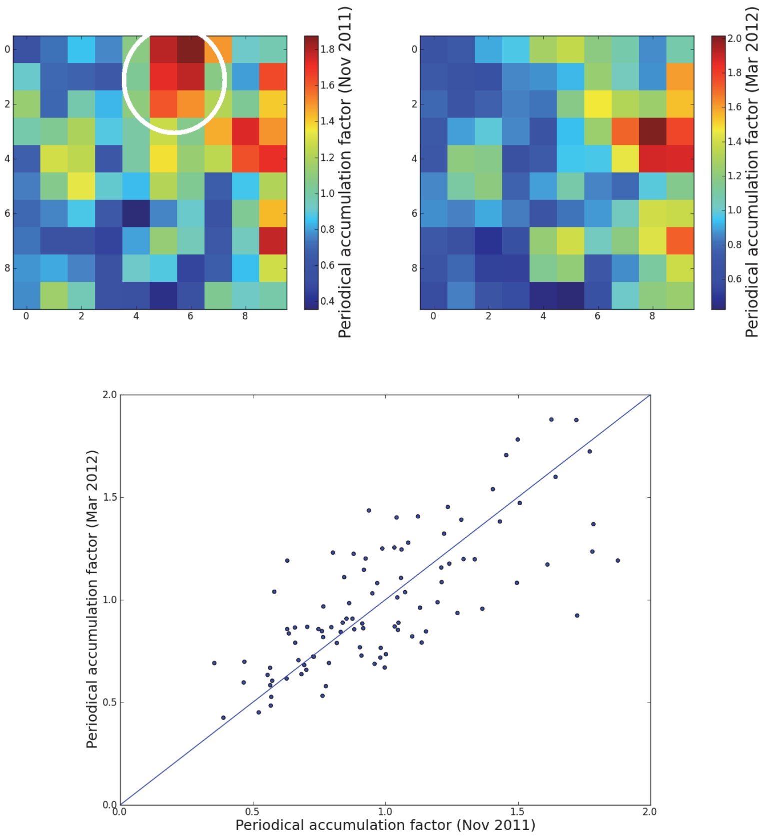

Fig. 7. The upper two images show the distributions of the periodical accumulation factors of two different snowmelt periods (November 2011 versus March 2012). The white circle in the upper left image (November 2011) shows an obvious difference from the upper right image (March 2012). The lower image shows a comparison between the periodical accumulation factors of November 2011 and March 2012.

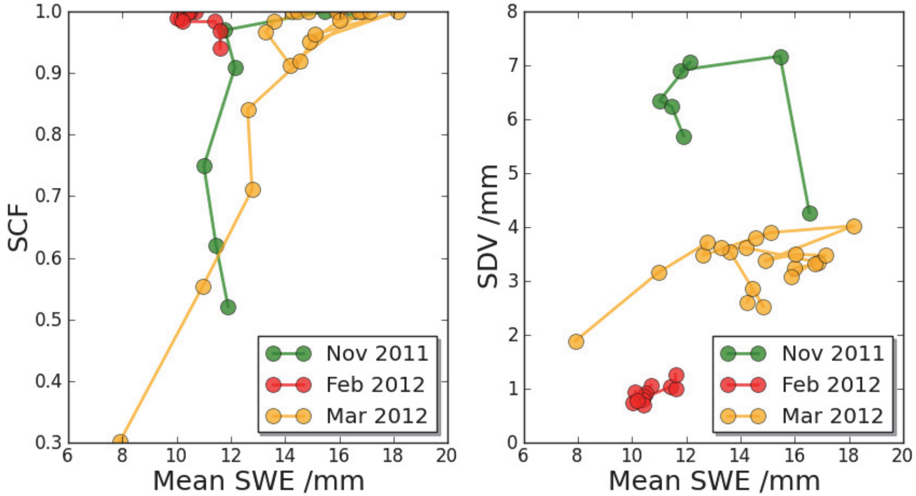

Fig. 8. The SCF versus the mean SWE (left) and the SDV versus the mean SWE (right) in three different periods. The SCF and SDV values were calculated from the field investigation results.

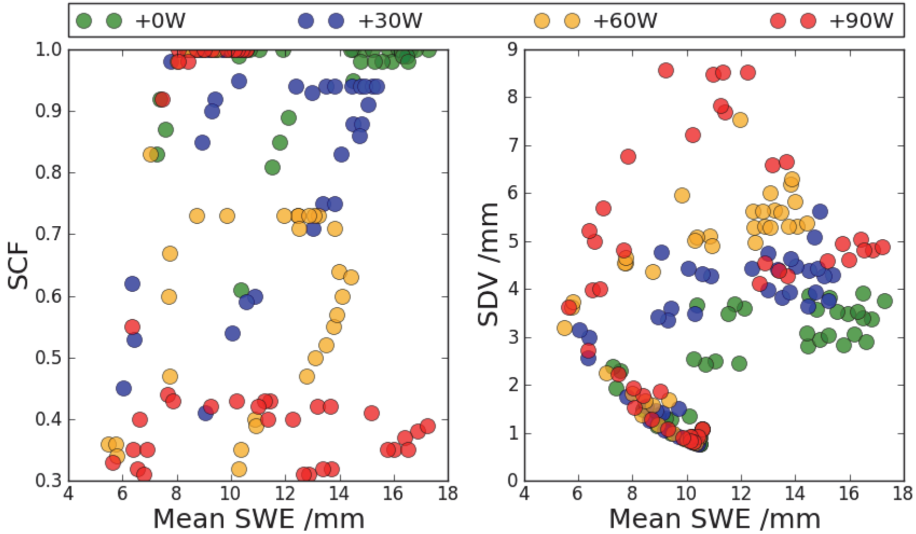

Fig. 9. The SCF versus the SWE (left) and the SDV versus the mean SWE (right) for different simulation scenarios. In these simulation scenarios, the hourly incoming shortwave radiation data increased by 30 W, 60 W and 90 W.

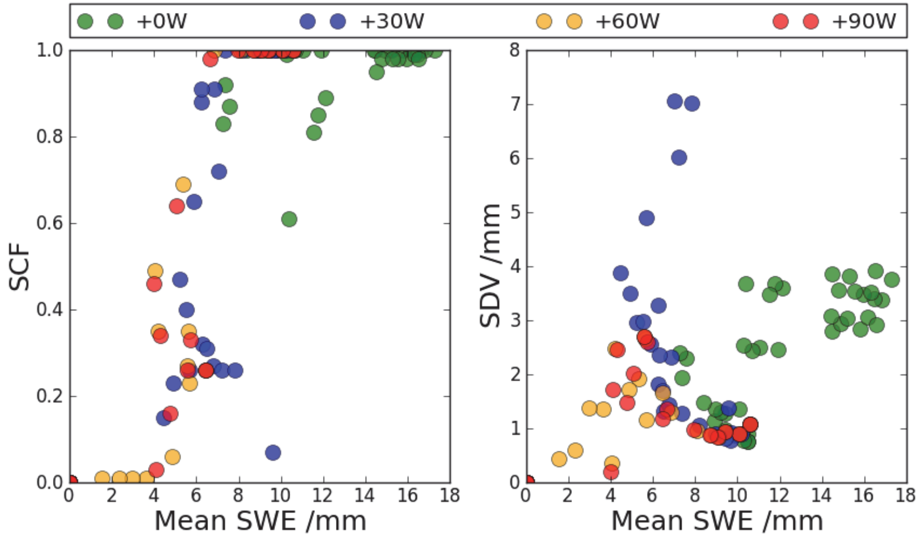

Fig. 10. The SCF versus the mean SWE (left) and the SDV versus the mean SWE (right) for the different simulation scenarios. In these simulation scenarios, the hourly incoming longwave radiation data increased by 30 W, 60 W and 90 W.

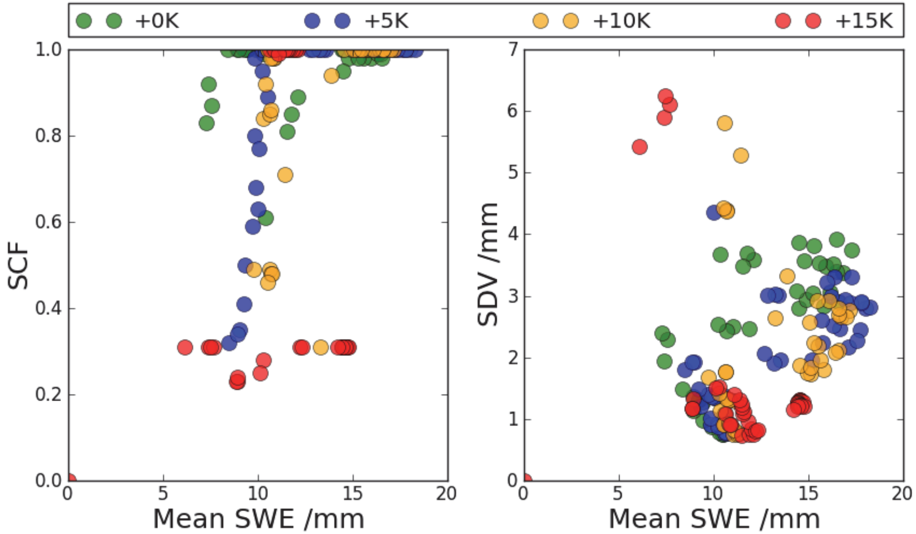

Fig. 11. The SCF versus the mean SWE (left) and the SDV versus the mean SWE (right) for the different simulation scenarios. In these simulation scenarios, the hourly air temperature data increased by 5 K, 10 K and 15 K.